Available online at www.sciencedirect.com
SCIENCE DIRECT®
Fire Safety Journal 39 (2004) 721–736
FIRE SAFETY JOURNAL
www.elsevier.com/locate/firesaf

The simulation of fire sprinklers thermal response in presence of water droplets ☆

Paolo Ruffino, Marino diMarzo*

Department of Fire Protection Engineering, University of Maryland at College Park, UMD, College Park 20742, USA

Received 29 November 2001; received in revised form 12 July 2004; accepted 13 July 2004
Available online 1 September 2004

Abstract

When a fire occurs, the sprinkler closest to the location of the fire typically activates first and releases water droplets into the rising plume of hot gases. Part of these droplets is entrained by the plume and may impact on adjacent sprinklers providing evaporative cooling and thus delaying their activation. The model of the thermal response of sprinklers in these conditions suggests the introduction of the concept of equivalent cylindrical links: a solid metallic cylinder is said to be equivalent to a given fire sprinkler link if it reaches the activation temperature of the sprinkler at the same time, both in dry conditions and in presence of water droplets carried by the hot gas flow. Tests are conducted on both fire sprinklers and equivalent cylindrical links to validate this theoretical approach. The results compare favorably both in dry and wet conditions for the range of parameters considered in this study. Therefore, this approach enables the transient quantification of the sprinkler thermal response in an actual fire scenario such as a large-scale fire test.

Keywords: Sprinklers; Evaporative cooling; Fire testing instrumentation

☆Part of this work was presented in a paper at the 7th IAFSS Symposium in Worcester, MA, in 2002.

*Corresponding author. Tel.: +1-3014055257; fax: +1-3014059383.
E-mail address: marino@eng.umd.edu (M. diMarzo).

0379-7112/$ - see front matter © 2004 Elsevier Ltd All rights reserved.
doi:10.1016/j.firesaf.2004.07.002

Nomenclature

A	sprinkler link cross-sectional area orthogonal to the flow, m^2
c	specific heat at constant pressure, $J\,kg^{-1}\,°C^{-1}$
d	simulated sprinkler link diameter, m
E	evaporative cooling parameter, $°C\,s\,m^{-2}$, see Eq. (5)
h	convective heat transfer coefficient, $W\,m^{-2}\,°C^{-1}$
k	thermal conductivity, $W\,m^{-1}\,°C^{-1}$
Pr	gas Prandtl number
Re	Reynolds number: $U\,d\,\nu_G^{-1}$
RTI	Response Time Index, $m^{1/2}\,s^{1/2}$
S	sprinkler link surface, m^2
t	time, s
T	temperature, °C
U	gas velocity, $m\,s^{-1}$
V	sprinkler link volume, m^3
$\dot{V}$	volumetric flow rate, $m^3\,s^{-1}$
x	coordinate along the duct, m
x_E	distance of complete evaporation from the point of water injection, m

Greek

β	water volumetric fraction
ΔT	asymptotic temperature difference, °C, see Fig. 2 and Eq. (9)
κ	collection efficiency
ρ	density, $kg\,m^{-3}$
Λ	latent heat of vaporization of water, $J\,kg^{-1}$
λ, ξ, γ, φ	constants, see Eqs (14) and (15)

Subscripts and Superscripts

0	initial time
A	sprinkler activation
D	dry condition
G	gas
L	liquid
r	reference value
S	sprinkler link
W	wet condition

Acronyms

ECSAT	Evaporative Cooling Sensor Accuracy Test (facility)
QR	Quick Response glass bulb sprinkler
SE	Solder Element sprinkler
SR	Standard Response glass bulb sprinkler

1. Introduction

Traditionally, the modeling of the sprinkler activation system is based on a lumped heat capacity energy balance for the sprinkler link [1,2]. According to this model (identified in the following as the *RTI* model), the hot gases, flowing under the ceiling, heat the sprinklers by convection. The time delay between the onset of the fire and the activation of a given sprinkler depends on the size of the link and the distance from the fire location, as well as on the intensity of the fire. A correction to the simple convective model can be introduced to take into account the heat lost by conduction from the sprinkler to its supporting pipe, as well as the radiative heat flux induced by the fire plume [3].

A model for estimating the evaporative heat loss due to the water spray introduced by a sprinkler in a smoke layer is reported by Chow [4]. The author points out that the water droplets evaporate while travelling through the smoke layer. This results in higher cooling and smaller air-drag effects. However, the water droplets may not be able to reach the burning objects. The model investigates the evaporation of the sprinkler water spray in the hot smoke layer, providing a scheme to evaluate the penetration of the water.

Studies on the interaction between a water spray generated by a sprinkler and smoke are important to improve the understanding of these complex processes and to provide effective design parameters for fire protection [5]. A model to simulate the interaction between a sprinkler water spray and a two-layer fire environment under arbitrary combinations of sprinkler elevation, upper and lower layer thickness and gas temperature is derived by Cooper [6]. The control of the temperature and thickness of the upper layer to sub-critical values could be useful to guarantee fire sprinkler operation without smoke accumulation in the fire compartment.

An understanding of the behavior of the fire plume and fire induced flow near the ceiling of a room is necessary to optimize the response time and the placement of the sprinklers. An experimental and theoretical study is developed by Alpert [7] to characterize natural convection associated with large fires where the flames are comparable in height to the ceiling. Recent experiments on warehouse fires indicate that the *RTI* model [1,2] is not always adequate to predict the response of an array of fire sprinklers. The model, indeed, appears to be accurate in simulating the behavior of the sprinkler closest to the fire, but fails to predict the response of the surrounding sprinklers. The cause for this deficiency is related to the presence of water droplets, which are sprayed onto the fire by the first activated sprinkler. Part of the water droplets released by the first sprinkler is entrained by the ascending fire plume and transported away. Some of these droplets may reach other sprinklers and deposit on their link. The consequent evaporation absorbs heat from the link, causing it to cool down. This cooling effect increases the time required by the sprinklers to activate and cannot be predicted by the original *RTI* model.

An improved model for the thermal response of the sprinkler has been developed and experimentally assessed at the Evaporative Cooling Sensor Accuracy Test (ECSAT) facility of the University of Maryland [8]. This model takes into account the evaporative cooling effect produced by water droplets contained in the gas

stream as they impact over the sprinkler surface. The purpose of this paper is to describe the thermal transient of fire sprinklers exposed to a gas flow laden with water droplets using an appropriately constructed equivalent cylindrical link.

2. ECSAT Facility description

Fig. 1 provides a sketch of the main portion of the ECSAT facility. A blower placed near the outlet of the duct generates the gas flow inside the system. The air entering into the duct (of square section, 0.61 m × 0.61 m) is heated up by a natural gas burner and then flows upward. A honeycomb structure, about 0.2 m thick and made of tightly packed steel wool, is placed in the initial portion of the duct. Its

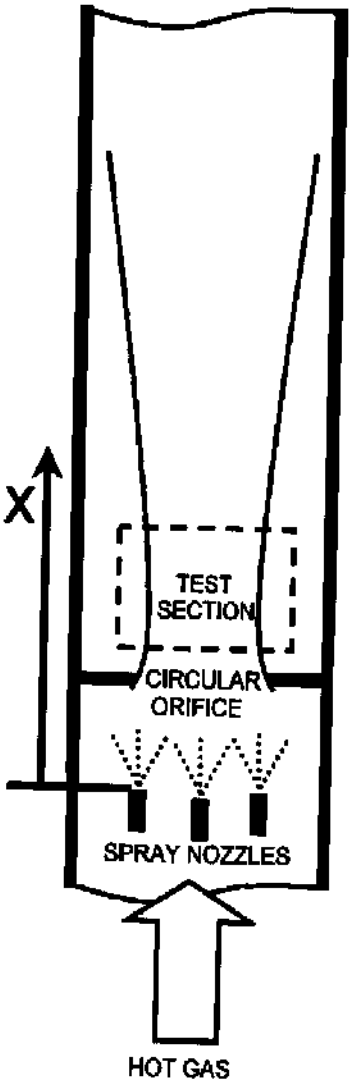

Fig. 1. Schematic of the ECSAT facility.

purpose is to spread the gas stream over the entire cross-section, as well as to obtain a uniform temperature distribution over the flow cross-section. As the hot gas emerges from the honeycomb, it reaches the water spray injection location. A finely atomized water spray is injected into the gas stream. A square-edged circular orifice (0.25 m diameter) is located 0.5 m downstream of the sprays. The orifice represents an abrupt restriction of the cross-sectional area for the two-phase flow. The orifice generates a vena contracta, which is characterized by a near parallel streamline profile.

At the location of the vena contracta, which occurs about 0.4 m downstream of the orifice, the mean velocity field is parallel to the axis of the orifice (no radial velocity component). The range of velocities investigated in this study is in between 3 and 9 m/s. For these values, the Reynolds number associated with the gas flow inside the duct is larger than 9000, indicating that the flow is turbulent upstream of the orifice. Additional turbulent effects at the vena contracta may also be induced by the gas jet produced by the orifice as it mixes with the slower gases flowing downstream. Clearly, the turbulence level in the test section and the disturbances induced by the gas jet affects the gas velocity field, in particular its alignment with the axis of the duct. Calculations [9] show that the intensity of turbulence, defined as the ratio of the fluctuating radial velocity to the mean gas velocity, is about 5% percent, which is not significant compared to other experimental uncertainties present in this study. Also, note that typically 300 particle samples are analyzed to obtain statistically meaningful velocity measurements, thus decreasing the inaccuracies associated with the turbulence level of the gas flow. Because of the one-dimensional characteristic of the flow field, the vena contracta is chosen as the test section for the sprinkler experiments. Downstream of the vena contracta, the flow spreads and returns to occupy the entire duct cross-section.

The ECSAT facility allows for the measurement of the following quantities, which are needed in order to determine the evaporative cooling parameter E:

- the gas velocity
- the axial temperature evolution in both dry and wet conditions.

Particle Tracking Velocimetry (PTV) provides the gas velocity measurements in the cross-section [10]. The test section is illuminated by a 600 mW Argon ion laser sheet. Thirty measurements are made to obtain a statistically meaningful value of the droplets velocity. Note that the droplets introduced in the gas flow have a maximum volumetric mean diameter of less than 100 μm. By balancing the gravitational and drag forces, within the Stokes' approximation, the droplets reach a terminal velocity with respect to the gas flow of about 0.24 m s^{-1} while the gas velocities are in excess of 3.5 m s^{-1}. Therefore, the measured droplets velocity lags the actual gas velocity by less than 4%. Neglecting this difference, we can assume that the PTV measurements provide the velocity of the gas stream. The uncertainty in the velocity measurements is about 10 percent.

Thirty-three thermocouples (type K, with accuracy of ±2 °C) are placed inside the duct along its axis, both before and after the test section, to measure the gas axial temperature distribution in the facility and monitor the conditions during the

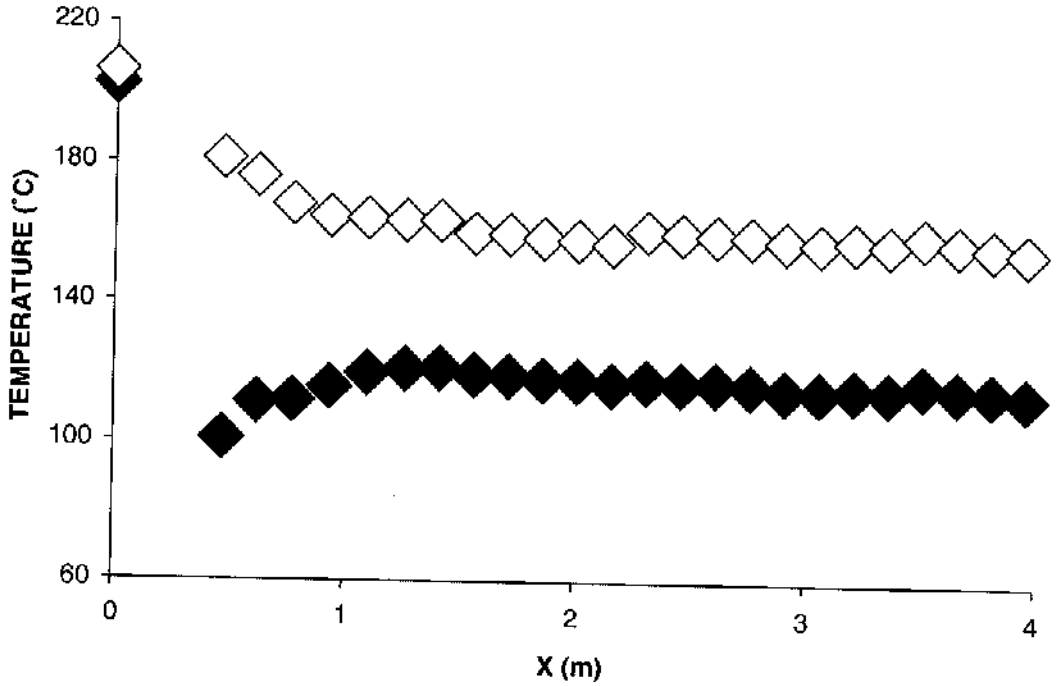

Fig. 2. Temperature evolution along the axis of the ECSAT facility: the open symbols identify a test in dry condition while the closed symbols refer to the very same test with addition of water droplets.

experiment. Fig. 2 reports the typical temperature axial evolution, for both dry and wet conditions. It can be observed that:

- due to the heat losses to the external environment, the gas temperature drops as the flow proceeds downstream the orifice.
- the gas temperature upstream the spray nozzle location is equal in both dry and wet conditions.
- About 2 m downstream the test section, the slope of the temperature distribution for the wet case matches the slope of the temperature distribution for the dry case. This indicates that the water is completely evaporated and the temperature is affected only by the heat losses to the environment.

Therefore, the thermocouples measure the gas temperature at the location before the sprays and at the location after the complete evaporation of the water. To determine the gas temperature between the sprays and the location of complete evaporation of the water, some information concerning the rate of vaporization of the droplets is needed.

3. Model formulation

A new model for the thermal response of a fire sprinkler link is derived to overcome the deficiencies of previous approaches [1,2]. In presence of water droplets,

the evaporative cooling term is proportional to the mass flow rate of the drops that deposit on the link surface. The following assumptions are made:

- the droplets in the gas stream are at the saturated liquid conditions. Therefore, the evaporative cooling per unit mass of water is equal to the latent heat of vaporization.
- the droplet distribution is uniform across any given flow cross-section.
- the water droplets are sparse in the hot gas flow, so that no droplet-droplet interactions are considered.
- only a portion of the droplets impacts the surface of the link, while some have sufficiently small inertia to move around the obstacle.
- all the water deposited on the link is assumed to evaporate.

In order to conduct the experiments in a controlled environment the primary sprinkler spray is simulated with a series of spray nozzles. These nozzles generate droplets of about 100 μm in diameter. The actual sprinkler heads typically generates a broad range of droplet sizes far exceeding 100 μm. However, consider that large droplets have terminal velocities that exceed the fire plume upward velocity. Therefore, they fall to the ground. Smaller droplets with moderate terminal velocity can be entrained by hot gasses toward the secondary sprinklers. Minute droplets will quickly evaporate in the stream. The droplets selected for this study are a reasonable compromise in size because they can easily move along with the gas while still being able to affect greatly the secondary sprinkler response. Another important aspect to consider is the relative humidity presence in the fire environment. Below the hot layer, one can consider the environment saturated. However the same air steam mixture transported in the hot layer will exhibit an extremely low relative humidity due to the sharp increase of the steam saturation pressure with temperature. This means that rapid vaporization will take place in the hot layer due to mass transfer.

The presence of the sprinkler affects the gas flow so that only a fraction of the water that would have passed through the cross-sectional area occupied by the link will actually deposit on it. We introduce the collection efficiency κ to represent the fraction of water that impacts the link. The impacting drops are assumed to evaporate on the link surface. This is reasonable because the droplets are small (their mean diameter is less than 100 μm) and sparse (the volumetric fraction is of the order of 10 ppm) and the gas temperature is high. Therefore, there is little chance for significant water build-up on the link, which may lead to run-off or re-entrainment of water in the gaseous stream. In fact, calculations show that the water volumetric fraction in the gas flow is too low to consider even remotely the possibility of water film formation over the cylinder surface. The evaporation rate of droplets over the cylinder surface is fast enough to completely vaporize the water before significant flooding occurs. Further, an experimental study by Grissom and Wierum [11] confirms that no flooding is likely to occur over the cylinder surface under any condition investigated in the present study. Correlations provided by Paleev and Filippovich [12] and Berry and Goss [13] indicate that any possible water build-up and consequential entrainment of water in the gas flow are negligible, as well. The

resulting energy balance can be written as:

$$\rho_S c_S V_S \frac{dT_S^W}{dt} = hS(T_G^W - T_S^W) - \rho_L U A \beta \kappa \Lambda, \tag{1}$$

The collection efficiency can be estimated by considering the Stokes' approximation applied to droplets carried by the gas stream over a cylinder in cross-flow [14]. In fact, the water droplets have a characteristic mean diameter of less 100 μm. The droplet Reynolds number, based on the droplet relative velocity to the gas, is less than 0.8 and the Stokes' approximation holds true. For the applications of concern, the collection efficiency approaches its asymptotic value of 0.97. Therefore, κ can be regarded as a constant in the applicable range of parameters.

The heat transfer correlation, for a cylinder in cross-flow, with a Reynolds number (based on the cylinder diameter) ranging between 40 and 1000 [15], yields the following dependence of the heat transfer coefficient on the relevant governing parameters:

$$h = 0.52 \frac{^kG}{d} Re^{0.5} Pr^{0.37}. \tag{2}$$

Note that, considering that the physical properties are almost constant, one can conclude that the heat transfer coefficient is proportional to the square root of the ratio U/d. Introducing the Response Time Index (RTI) and the Evaporative cooling parameter (E), by considering Eq. (2), we obtain:

$$RTI = \frac{\rho_S c_S V}{S} \frac{\sqrt{U}}{h} \tag{3}$$

$$E = \frac{\rho_L A \kappa \Lambda}{S} \frac{\sqrt{U/d}}{h}. \tag{4}$$

This means that the RTI is proportional to $\rho_S c_S d^{1.5}$ while the Evaporative cooling parameter is a constant quantity. With these new parameters, Eq. (1) can be rewritten as:

$$\frac{dT_S^W}{dt} = \frac{\sqrt{U}(T_G^W - T_S^W)}{RTI} - \frac{EU\beta\sqrt{d}}{RTI} \tag{5}$$

This equation can be integrated with the initial condition $T_S = T_0$ (at $t = 0$) to yield:

$$T_S^W = T_G^W - E\beta\sqrt{Ud} + \left(T_G^W - T_0 - E\beta\sqrt{Ud}\right) \exp\left(-\frac{\sqrt{U}}{RTI} t\right). \tag{6}$$

Eq. (6) provides the solution for the thermal response of a sprinkler link in presence of a flow of hot gases and water droplets. The value of the evaporative cooling constant E will be determined in the following. Note that, if no water is present in the flow (i.e. $\beta = 0$), the solution reduces to that provided by the RTI model:

$$T_S^D = T_G^D - (T_G^D - T_0) \exp\left(-\frac{\sqrt{U}}{RTI} t\right) \tag{7}$$

Consider the energy balance written for the airflow as:

$$\rho_G \dot{V}_G c_G (T_G^D - T_G^W) = \rho_L \dot{V}_G (\beta_0 - \beta) \Lambda. \tag{8}$$

The asymptotic temperature difference ΔT, between the two traces in Fig. 2, is associated with the sensible heat removed from the air in order to vaporize the droplets. It can be expressed in the following form:

$$\Delta T = \frac{\rho_L \beta_0 \Lambda}{\rho_G c_G}. \tag{9}$$

With Eq. (9), Eq. (8) can be simplified as:

$$T_G^D - T_G^W = \Delta T[1 - f(x)]. \tag{10}$$

The functional $f(x)$ relates the initial volumetric fraction to its evolution along the duct.

Eq. (1), written for a sensor wetted by water droplets yields a direct relationship between the convective heat transfer to the sensor and the latent heat associated with the vaporization of the droplets that deposit over its surface. At steady state, Eq. (1) simplifies as:

$$hS(T_G^W - T_S^W) = \rho_L U A \beta \kappa \Lambda. \tag{11}$$

Considering the volumetric fraction evolution during the evaporation process and using Eq. (4), Eq. (11) can be rearranged as:

$$T_G^W - T_S^W = E\sqrt{Ud}\beta_0 f(x). \tag{12}$$

By adding Eqs. (10) and Eq. (12), one finds that the functional $f(x)$ can be expressed in the following form:

$$f(x) = \frac{T_G^D - T_S^W - \Delta T}{E\sqrt{Ud}\beta_0 - \Delta T}. \tag{13}$$

Note that $f(x)$ is equal to 1 at the spray nozzles location and is equal to zero for x greater or equal to x_E, where all the water drops are evaporated. The D^2 law [16] suggests the following form of the functional:

$$f(x) = \begin{cases} \left(1 - \frac{x}{x_E}\right)^{\lambda} & x \leqslant x_E \\ 0 & x > x_E \end{cases}. \tag{14}$$

By plotting $T_G^D - T_G^W - \Delta T$ vs x one easily determines the value of x_E. Then limiting the data to the evaporative range and normalizing the abscissa as x/x_E, one can look at these data in a logarithmic plot and deduce the exponent λ of Eq. (14). The value of this exponent is found to be 1.7 for all the data considered. Note that the D^2 law yields an exponent equal to 1.5. This difference can be explained if one takes into account the expansion of the jet downstream the circular orifice (see Fig. 1). By continuity, this expansion produces a sharper decrease in the volumetric fraction than the one would observe in a constant cross-section flow configuration.

Finally, with the exponent and the evaporation distance known, one can determine the value of the evaporative cooling parameter E for all the tests. This is easily done fitting the wet condition data using Eq. (13) where the only fitting parameter available is indeed E. To facilitate this process, the temperature in dry conditions is represented with an exponential fit of the available data in the following form:

$$T_G^D(x) = (T_N - \xi)e^{-\gamma x} + \varphi x + \xi. \tag{15}$$

The constant φ represents the slope of the trace on the right side of the plot in Fig. 2 due to the heat transfer losses to the ambient.

Note that the volumetric fraction at the nozzles is evaluated considering the water and air volumetric flow rates, respectively. The database used to determine the value of the evaporative cooling parameter encompasses tests with:

- velocity ranging from 3 to 7 m s^{-1}
- gas temperatures at the nozzle locations between 150 and 250 °C
- volumetric fractions at the nozzles up to 19 ppm.

The numerical value of the evaporative cooling constant E, for all the tests considered here, is equal to $82 \pm 9 \times 10^6$ K s$^{1/2}$ m^{-1}.

The water volumetric fraction along the axis of the ECSAT facility is evaluated making use of the previous results as:

$$\beta = \beta_0 \left(1 - \frac{x}{x_E}\right)^{1.7} \text{ for } x \leqslant x_E. \tag{16}$$

These results are validated independently by direct measurements of the gas temperature and of the volumetric fraction obtain with novel instrumentation [17].

4. Sprinkler phenomenology

Solder-type sprinklers activate upon the melting of a metal alloy as it reaches a specific temperature. Various combinations of levers, struts and linkages are used to reduce the force acting on the solder. This minimizes the response time by reducing the mass of fusible metal to be heated. The solder material used for automatic sprinklers is an alloy composed principally of tin, lead, cadmium and bismuth.

A second type of sprinkler utilizes a frangible bulb. The small bulb of glass contains a liquid that does not completely fill the bulb, leaving a small gas bubble entrapped in it. As the liquid is heated up, the pressure increases leading to the shattering of the glass bulb thus activating the sprinkler.

In the ECSAT facility, these devices can be tested under combinations of gas temperature, gas velocity and water volumetric fraction. The ranges are: 100–250 °C, 3–9 m/s and 1–10 ppm, respectively, for the temperature, velocity and volumetric fraction. The sprinkler is mounted on a supporting frame through a Teflon insert that minimizes the heat losses by conductive heat transfer. The supporting frame

Table 1
Test conditions

	Condition A	Condition B
Gas temperature in dry conditions (°C)	146–149	208–210
Gas temperature in wet conditions (°C)	132–137	182–186
Initial & ambient temperature (°C)	25–30	32–33
Gas velocity ($m\,s^{-1}$)	4.4–4.6	3.7
Water volumetric fraction (ppm)	2	3.7–4

(constituted of an enclosed steel pipe) is filled with pressurized air. The sprinkler is suddenly exposed to the steady state flow in the ECSAT facility duct at the test section location identified in Fig. 1. The time of activation is measured by the operator from the very moment the sprinkler link enters the test section to the moment the air pressure inside the pipe collapses indicating the activation of the sprinkler. This measurement technique is similar to the one used in the plunge test [18]. Each test is repeated ten times to obtain a statistically meaningful value of the activation time, both in dry and wet conditions.

In the series of tests reported in this paper, the Solder Element sprinkler (SE), the Standard Response glass-bulb sprinkler (SR) and the Quick Response glass-bulb sprinkler (QR) are tested. Two different conditions have been selected. One (condition A) is a combination of low temperature, high velocity and low water content in the gas flow, while in the other (condition B) the gas temperature has been increased significantly and the gas velocity decreased. One water spray nozzle has been used in condition A, two nozzles are used in condition B. Table 1 summarizes the test conditions. As one may notice in Table 1, some properties have been given as a range of values since the experiments have been performed in different days. In particular, the climatic variations are reflected in the range of the initial ambient temperature.

5. Design of equivalent cylindrical links

In the following, the procedure to determine the size and material of an equivalent cylindrical link capable of simulating the behavior of a sprinkler link exposed to a gas flow laden with water droplets is described. A cylinder is said to be equivalent to a given sprinkler link if it reaches the activation temperature T_A in the same amount of time t_A, both in dry and wet condition, under any combination of gas temperature, gas velocity and water volumetric fraction.

The size and material of the simulated sprinkler link are chosen accordingly to the results shown hereafter. From the *RTI* model, described in Eq. (7), one obtains the expression:

$$RTI = \frac{t_A^D \sqrt{U}}{\ln((T_G^D - T_0)/(T_G^D - T_A))}. \tag{17}$$

Eq. (6), written at the time of activation, provides an expression for the equivalent cylindrical link diameter as:

$$d = \frac{1}{U}\left[\frac{1}{\beta E}\frac{T_G^W\left[1-\exp\left(t_A^W\sqrt{U}/RTI\right)\right]+T_A\exp\left(t_A^W\sqrt{U}/RTI\right)-T_0}{1-\exp\left(t_A^W\sqrt{U}/RTI\right)}\right]^2. \quad (18)$$

The temperature T_G^D and T_G^W are the gas temperature at the test section, in dry and wet condition respectively. T_G^D is measured by a thermocouple exposed to the hot gases in absence of water; T_G^W is calculated from Eq. (10) analyzing the temperature profiles in dry and wet conditions as previously mentioned.

The heat capacity of the equivalent cylindrical link is given by Eq. (3) in the form:

$$\rho_S \cdot c_S = \left(\frac{d_r}{d}\right)^{1.5}\frac{RTI}{RTI_r}(\rho_S \cdot c_S)_r. \quad (19)$$

In this equation, an aluminum cylinder is used as the reference cylinder with $d_R = 6.4$ mm. Its *RTI* has been determined experimentally to be 100 $(\mathrm{m\,s})^{1/2}$

The experiments on commercial sprinklers provide the *RTI* representative of any given sprinkler type using Eq. (17). The size of the equivalent cylindrical sprinkler link and its material are evaluated through Eqs. (18) and (19). For the sprinklers tested, we found that:

- For the SE sprinkler the heat capacity is equal to 2710 $\mathrm{kJ\,m^{-3}\,K^{-1}}$.
- For the SR sprinkler the heat capacity is equal to 2740 $\mathrm{kJ\,m^{-3}\,K^{-1}}$.
- For both the SE and SR sprinklers the equivalent diameter is between 6 and 7 mm.

To represent both these sprinklers we decided to use a 6.7 mm diameter cylinder made of zinc, which has a heat capacity of 2780 $\mathrm{kJ\,m^{-3}\,K^{-1}}$.

- For the QR sprinkler the heat capacity is equal to 2240.
- For the QR sprinkler the equivalent diameter is about 4 mm.

To represent this sprinkler we decided to use aluminum, which has a heat capacity of 2440 $\mathrm{kJ\,m^{-3}\,K^{-1}}$. This value is somewhat higher than the sprinkler heat capacity. Considering Eq. (19), while maintaining the same *RTI*, it follows that one should reduce the equivalent cylindrical link diameter. Therefore, a 3.7 mm diameter has been selected.

The equivalent cylindrical links are inserted in the test section in conditions identical to those of the corresponding sprinkler tests and the temperature evolution, measured by a thermocouple positioned at the center of the cylinder, is recorded.

6. Results

Table 2 summarizes the results for the various sprinklers used in the study. The activation time of the sprinklers is given as the average value plus or minus one

standard deviation, calculated from ten plunge tests. Note that the time of activation in wet condition is about twice the time measured in absence of water and also that the standard deviation is larger for the wet condition tests.

Table 2
Results

	Condition A	Condition B
RTI for sprinkler SE ($m^{1/2}s^{1/2}$)	100	98
SE sprinkler activation time in dry conditions measured (s)	21.4±2.4	13.7±1.4
SE sprinkler activation time in wet conditions measured (s)	35.0±2.6	27.1±1.8
Temperature of activation SE (°C)	72	
RTI for sprinkler SR ($m^{1/2}s^{1/2}$)	110	109
SR sprinkler activation time in dry conditions measured (s)	23.2±2.3	13.1±1.7
SR sprinkler activation time in wet conditions measured (s)	41.8±6.2	24.0±2.6
Temperature of activation SR (°C)	68	
RTI for sprinkler QR ($m^{1/2}s^{1/2}$)	42	44
QR sprinkler activation time in dry conditions measured (s)	8.0±1.5	4.5±1.2
QR sprinkler activation time in wet conditions measured (s)	12.4±3.1	8.1±1.5
Temperature of activation QR (°C)	68	

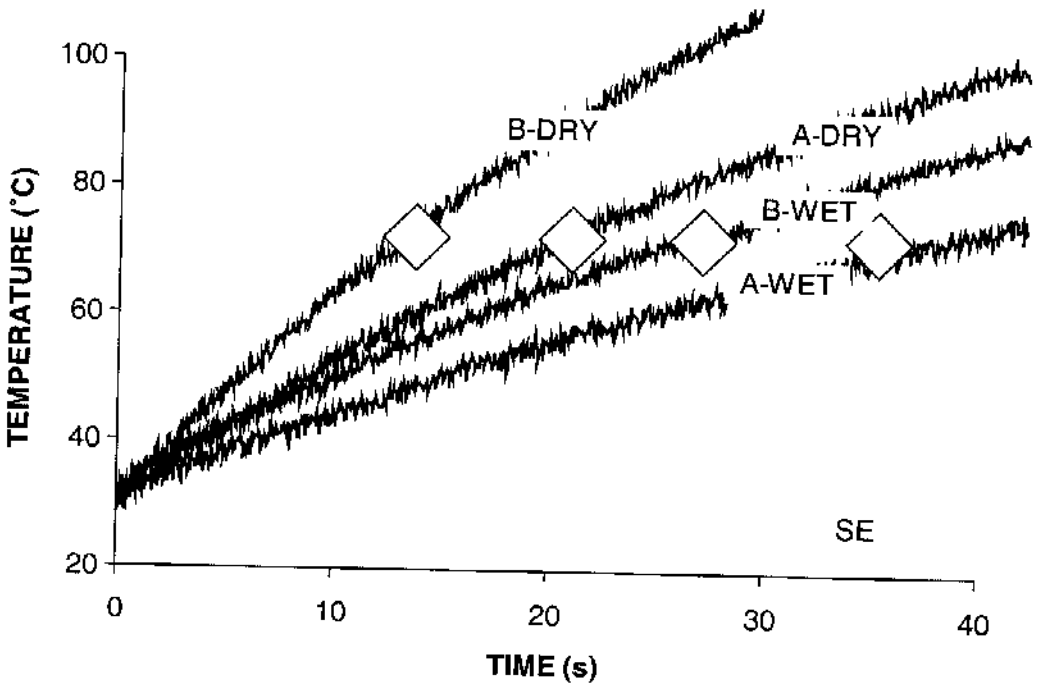

Fig. 3. Comparison of the thermal response of the equivalent cylindrical link (zinc, 6.7 mm in diameter) and of SE sprinklers: the open symbols identify the sprinkler activation times for the different conditions labeled in the figure (e.g. "A-DRY" means condition A without water droplets).

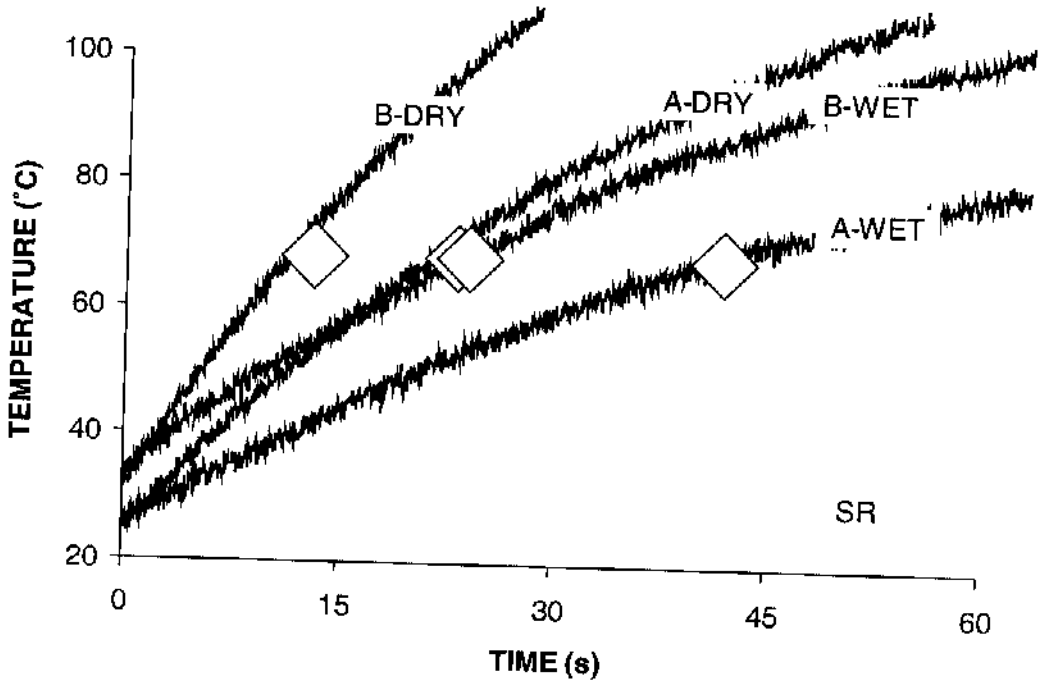

Fig. 4. Comparisons of the thermal response of the equivalent cylindrical link (zinc, 6.7 mm in diameter) and of SR sprinklers: the open symbols identify the sprinkler activation times for the different conditions labeled in the figure (e.g. "B-WET" means condition B with water droplets).

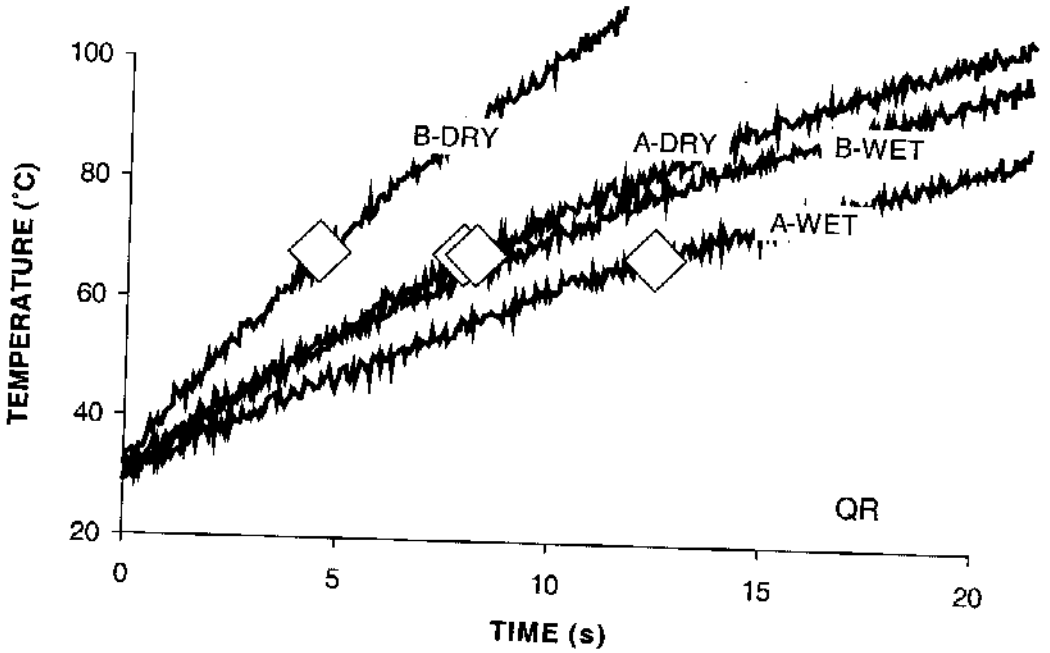

Fig. 5. Comparison of the thermal response of the equivalent cylindrical link (aluminum, 3.7 mm in diameter) and of QR sprinkler: the open symbols identify the sprinkler activation times for the different conditions labeled in the figure (e.g. "A-WET" means conditions A with water droplets).

Figs. 3–5 report the measured temperature evolution of the equivalent cylindrical links. Also, the values of the measured activation time for the sprinklers are identified in the plots. It can be observed that, in each situation, the equivalent cylindrical link behaves like the corresponding sprinkler, well within the accuracy of the measurements that are listed in Table 2. The important contribution of the equivalent cylindrical link concept is the description of the continuous temporal evolution of the thermal response rather than the simple binary information provided by the sprinkler (activated/non-activated). Further, this experimental tool used in a large-scale test can provide a superior description of the thermal phenomena and thermal history leading to the activation of sprinklers in presence of water droplets or in dry conditions.

7. Conclusions

The evaporative cooling model has been used to simulate the behavior of a given commercial sprinkler under any condition through appropriate cylindrical sensors. Three different sprinkler types have been tested in both dry and wet condition, for two completely different situations. The correspondent simulated sprinkler links have been tested in the same conditions used for sprinklers. The results compare favorably. This proves the capability of the equivalent cylindrical links to simulate sprinklers thermal behavior under any circumstance and may enable the monitoring of the thermal excursion of sprinklers by inferring their behavior from the data collected with this kind of sensors positioned in proximity of the actual sprinkler.

Acknowledgements

The Building and Fire Research Laboratory of the National Institute of Standards and Technology provided the financial support for this research.

References

[1] Heskestad G, Smith HF. Investigation of a new sprinkler sensitivity approval test: the plunge test FMRC 22485, Factory Mutual Research Corporation, Norwood, MA, 1976.
[2] Heskestad G, Bill RG. Modeling of thermal responsiveness of automatic sprinklers. Fire Safety Science—Proceedings Second International Symposium, 1988. p. 603–612.
[3] Yao C. Overview of sprinkler technology research. In: Curtat MR, Bodart XI, editors. Fire Safety Science—Proceedings fifth International Symposium. Bethesda MD: IAFSS; 1999. p. 93–110.
[4] Chow WK. On the effect of a sprinkler water spray. Fire Technology 1989;25:364–73.
[5] Chow WK, Tao B. Numerical modeling for interaction of water spray withsmoke layer. Numerical Heat Transfer Part A 2001;39:267–83.
[6] Cooper LY. The interaction of an isolated sprinkler spray an a two-layer compartment fire environment. Int J Heat Mass Transfer 1995;38:679–90.
[7] Alpert RL. Calculation of response time of ceiling-mounted fire detectors. Fire Technology 1972;8:181 95.

[8] Ruffino P, diMarzo M. The effect of evaporative cooling on the activation time of sprinklers. Fire Safety Science–Proceedings Seventh International Symposium, 2003. p. 481–492.
[9] Brodkey RS. The phenomena of fluid motions. NewYork: Dover Publications Inc; 1995.
[10] Adrian RJ. Particle-imaging techniques for experimental fluid mechanics. Annu Rev Fluid Mech 1981;23:261–304.
[11] Grissom WM, Wierum FA. Liquid spray cooling of a heated surface. Int J Heat Mass Transfer 1981;24:261–71.
[12] Paleev II, Filippovich BS. Phenomena of liquid transfer in two-phase dispersed annular flow. Int J Heat Mass Transfer 1966;9:1089–93.
[13] Berry MR, Goss WP. An integral analysis of condensing annular-mist flow. AIChE J 1972;18:754–61.
[14] Aihara T, Fu WS. Effect of droplet-size distribution and gas-phase flow separation upon inertia collection of droplets by bluff-bodies in gas-liquid mist flow. Int J Multiphase Flow 1986;12:389–403.
[15] Zaukauskas A, Ziugzda J. Heat transfer of a cylinder in cross-flow. Washington, DC: Hemisphere Publishing Corporation; 1985.
[16] Kanuri AM. Introduction to combustion phenomena. London: Gordon and Breach; 1972.
[17] Ruffino P, diMarzo M. Temperature and volumetric fraction measurements in a hot gas laden with water droplets. J Heat Transfer 2003;125:356–64.
[18] Standard for automatic sprinklers for fire-protection service, UL 199, 8th ed. Underwriters Laboratories, Inc, 1992.